Subsarcomeric distribution of calcium in demembranated fibers of rabbit psoas muscle

M. E. Cantino,* T. StC. Allen,‡ and A. M. Gordon‡

*Department of Physiology and Neurobiology, University of Connecticut, Storrs, Connecticut 06269; and ‡Department of Physiology and Biophysics, University of Washington, Seattle, Washington 98195 USA

ABSTRACT Direct measurements were made of the Ca distribution within sarcomeres of glycerinated rabbit psoas muscle fibers in rigor using electron probe x-ray microanalysis. Both analogue raster analysis and digital x-ray imaging were used to quantitate the Ca distribution along thick and thin filaments as a function of the concentration of free Ca^{2+}. Even when corrected for the estimated contribution of Ca bound to thick filaments, the Ca measured in the region of overlap between thick and thin filaments significantly exceeded the Ca in the I-band at subsaturating concentrations of free Ca^{2+}. At saturating levels of free Ca^{2+}, the excess Ca in the overlap region was diminished but still statistically significant. The data thus suggest that the formation of rigor linkages exerts multiple effects on the binding of Ca^{2+} to thin filaments in the overlap region by increasing the affinity of troponin C for Ca^{2+} and possibly by unmasking additional Ca^{2+} binding sites. The data also show that the cooperativity invested in the thin filaments is insufficient to permit the effects of rigor cross-bridge formation on Ca^{2+} binding to propagate far along the thin filaments into the I-band.

INTRODUCTION

Elevation of myoplasmic free Ca^{2+} leads to the generation of contractile force in both skeletal and cardiac muscle. For a number of years, troponin has been considered to be the primary Ca^{2+}-sensitive switch regulating actomyosin interaction in striated muscle (Ebashi and Endo, 1968). Calcium binding to troponin, however, may itself be modulated by actomyosin interaction. Such modulation was first reported by Bremel and Weber (1972), who investigated the effects of rigor complexes on Ca^{2+} binding to regulated thin filaments in both myofibrils and reconstituted actomyosin preparations. In these systems, troponin appeared to have a higher affinity for Ca^{2+} in the presence than in the absence of rigor linkages.

Several subsequent studies have further investigated the effects of actomyosin interaction on the regulatory proteins in fibers. For example, Fuchs and co-workers reported an increase in the number of Ca^{2+} binding sites with rigor cross-bridge formation (Fuchs, 1977*a, b,* 1978), but not with increased force, in skinned skeletal muscle (Fuchs, 1985; Fuchs and Wang, 1991). In cardiac muscle, Pan and Solaro (1987) reported greater binding of Ca^{2+} to thin filaments in the absence of than in the presence of ATP only at submaximal Ca^{2+} levels in cardiac muscle. Hofmann and Fuchs (1987) found that the amount of Ca^{2+} binding to the thin filament increased with sarcomere length on the ascending limb of the cardiac muscle force-length relationship. This effect was attributed to differences in the number of attached cross-bridges. Evidence for effects of cross-bridge interactions on Ca^{2+} binding to troponin C (TnC) can also be found in the studies of Ridgway and Gordon (1984) and Allen and Kurihara (1982). These researchers observed that sudden detachment of cross-bridges leads to increased myoplasmic free Ca^{2+} and concluded that the detachment of cross-bridges reduces the Ca^{2+}-affinity of troponin. Recent studies with fluorescent derivatives of troponin subunits provide a possible mechanism for alterations in Ca^{2+} binding by demonstrating that cross-bridge formation produces structural changes in the vicinity of the probe (Trybus and Taylor, 1980; Guth and Potter, 1987; Gordon et al., 1988).

In this study, we sought to exploit the spatial resolution of electron probe x-ray microanalysis (EPXMA) to understand more fully the effect of actomyosin interaction on binding of Ca^{2+} to thin filaments in fibers. In 1982, Somlyo and co-workers (Kitazawa et al., 1982) obtained with EPXMA of skinned skeletal muscle fibers direct evidence that Mg is bound to thin filaments in the I-band at pCa $\approx$ 9 and that Ca displaces this Mg at pCa $\approx$ 5. The authors estimated that 3–4 mol Ca bound to 1 mol of troponin at pCa $\approx$ 5. These authors, however, did not attempt to determine the distribution of Ca along the entire thin filament.

Our aim in applying EPXMA to the study of Ca^{2+} binding in fibers was twofold. We wished to determine whether the resolution offered by EPXMA is sufficient to determine the Ca distribution within single sarcomeres. Moreover, by examining the distribution of Ca along the length of thin filaments, we wished to test two hypotheses. The first hypothesis, which arises from the studies of Fuchs, is that rigor cross-bridges unmask an additional Ca^{2+} binding site per TnC in the overlap region of the sarcomere. By performing EPXMA of fibers ultrarapidly frozen in rigor solutions containing saturating and subsaturating concentrations of free Ca^{2+}, we sought to discriminate an unmasking of additional Ca^{2+} binding sites from an increase in Ca^{2+} affinity. The second hypothesis is that the effects of rigor cross-bridges on Ca^{2+} binding are limited in spatial spread along the thin filament. This hypothesis rests on Wegner and Walsh's (1981) analysis of troponin I–troponin T interactions. The analysis indicated that the average number of sequential regulatory units in the same state is $\approx$3 in par-

0006-3495/93/01/211/12 $2.00

TABLE 1 **Solution composition**

Solution	Concentration								
						MgP_2*		CaP_2*	
	NaP*	Na_2EGTA	MOPS	Na_2ATP	Na_2CP	Total	Free	Total	Free
				mM				*μM*	
Relaxing	130.1	11.1	103.9	3.3	15.6	5.0	1.0	5.2	—
Rigor, pCa									
9.05	130.0	11.1	201.7	—	—	1.4	1.0	39.0	0.009
6.25	130.0	0.0333	253.0	—	—	1.0	1.0	23.4	0.6
5.67	130.0	0.0281	253.0	—	—	1.0	1.0	27.3	2.1
5.31	130.0	0.0286	253.0	—	—	1.0	1.0	29.3	4.9
4.76	130.0	0.0179	253.0	—	—	1.0	1.0	35.1	17.4
4.30	130.0	—	252.6	—	—	1.0	1.0	50.1	50.1

* P is propionate ion.

tially activated conditions. In contrast, studies by Brandt and co-workers (1984*a, b;* 1987) on the cooperativity in the relation between tension and Ca or MgATP concentrations led to a proposal that all 26 troponin-tropomyosin units in a regulatory strand make a concerted, cooperative transition from the inhibitory to the disinhibitory position. EPXMA measurements provide an opportunity to examine whether cooperativity in the thin filament allows cross-bridge attachments in the overlap region to exert long range effects on Ca distributions between the A-I junction and the Z line.

METHODS

Preparation of glycerinated fiber bundles

New Zealand white rabbits were killed with an intravenous injection of sodium pentobarbitol. The psoas major muscles were isolated and cooled to 5–10°C. Bundles of psoas muscle, 1 mm diameter, were isolated, tied to wooden sticks, and stored at 4°C for 24 h in a skinning solution containing (mM) 100 KCl, 9.0 MgCl, 4.0 Na_2 ATP, 5.0 ethyleneglycol-bis(β-aminoethyl ether)-*N,N,N,N*-tetraacetic acid (K_2EGTA), 10 3-(n-morpholino) propanesulfonic acid (MOPS), pH 7.00, and 50% vol/vol glycerol. After 24 h, the solution bathing the bundles was replaced with fresh skinning solution, and the bundles were stored at −20°C for ≥2 wk. For each experiment, a flat strip of 10 or so fibers was isolated from the larger bundles. Immediately after dissection, the fiber bundle was placed in a relaxing solution containing 0.5% wt/wt 3-[(3-Cholamidopropyl)dimethylammonio]-1-propanesulfonate (CHAPS) for 20 min and then returned to the standard relaxing solution (Table 1).

Induction of rigor and freezing of fiber bundles

Two modifications were made to the usual bathing solutions for glycerinated fibers to improve Ca detection and to reduce ambiguity of EPXMA data (Kitazawa et al., 1982). First, the bathing solutions (Table 1) contained Na^+ as the major cation to eliminate any error associated with incomplete separation of the potassium K_β and calcium K_α x-ray peaks. The Ca^{2+}-dependence of tension development and the maximal isometric tension of fibers bathed in solutions with Na^+ as the major cation do not differ from those of fibers bathed in solutions with K^+ as the major cation (Gordon et al., 1973; Fink et al., 1986). Second, since EPXMA measures total Ca (bound plus free), the total Ca in solution was kept low (23–50 μM, as assayed with atomic absorption spectroscopy). This level of Ca contributes a maximum of 0.28 mmol/kg dry wt in a dry cryosection (assuming 85% hydration in the I-band region before drying), which is below the threshold for detection of Ca by EPXMA with our equipment (~0.4 mmol/kg dry wt). Solutions with differing free Ca^{2+} concentrations were prepared by varying total EGTA. Solution makeup was calculated using a computer program, taking into account the binding constants of ATP (O'Sullivan and Smithers, 1979) and EGTA (Martell and Smith, 1974, 1982) for the various constituent ions in the bathing solutions, corrected for pH (Phillips et al., 1963; Ellis and Morrison, 1982), temperature (Khoo et al., 1977), and ionic strength (Phillips et al., 1966; Khoo et al., 1977). Ionic strength for all solutions was 0.19 M. Table 1 shows the composition of the solutions used in these experiments.

After treatment with CHAPS, fiber bundles were transferred to the transducer setup. Fibers were attached at one end to a force transducer and at the other end to a mechanical stage used to adjust sarcomere length to 3.2 μm in relaxing solution (shortening to ~3.0 μm in rigor solution). Attachment was effected in some cases by using aluminum T clips and in others by wrapping the bundle around small wire hooks (30 μm diameter) that had been treated with abrasive to prevent slippage. The force transducer was a photoelectric displacement measuring device modified after Chui et al. (1982). Bathing solutions were placed in troughs milled into a block of Plexiglas mounted on a spring loaded stage. Once attached to the apparatus, the fiber bundle could be immersed in bathing solution pools and transferred from one pool to another by lowering the spring-loaded stage and moving a new pool into position (Hellam and Podolsky, 1969). Each pool contained 2 ml of bathing solution, which was kept covered to prevent evaporative loss of solutions. The bottoms of the bathing pools were made of clear Plexiglas, which allowed the bundle to be illuminated from below. Sarcomere length was measured by illuminating the bundle with a 5-mW HeNe laser and monitoring the resulting diffraction pattern with a calibrated translucent grid placed above the fiber. Once the experimental condition had been established (after ≥20 min in the final bath to ensure diffusion throughout the bundle), the bundle was raised out of the bath, touched at one end with filter paper to remove excess solution, and clamped with copper-clad pliers cooled in liquid nitrogen. Time between removal from pool and freezing was 5–10 s.

Preparation of freeze-dried cryosections

Frozen fibers were mounted on metal chucks with a low temperature glue (*s*-butyl benzene), and sections of ~100 nm in thickness were cut at between −100 and −120°C with glass knives at clearance angles of 7°. Dry cut sections were transferred to formvar and carbon-coated folding grids with an eyelash probe and were pressed between the two halves of the folded grid with a cold metal rod. The closed grids were vacuum freeze-dried overnight and stored in a desiccator before analysis.

Collection and processing of spectral data: analogue raster and digital image analysis

The principles behind the technique of EPXMA have been described in detail elsewhere (e.g., Hall and Gupta, 1982; Johnson and Cantino, 1986; Somlyo et al., 1989). Only those details pertaining to this study will be described here. Data were collected in scanning transmission mode in a microscope (model 1200EX; JEOL USA Inc., Peabody, MA) equipped with an x-ray detector (30 mm^2 Si(Li); Link Systems, Reston, VA) and an analytical system (model AN10000; Link Systems). Two modes of spectral collection were used in this study. In the first mode, referred to here as analogue raster analysis, the scanning raster was positioned by the operator in a given location, and x rays were collected for 500 s. The second mode was digital analysis, in which the field was selected by the operator but the location of the beam within that field was controlled by a microprocessor, which positioned the beam at points in a prespecified matrix. At each pixel, a spectrum was gathered and processed to yield a series of values representing the number of x rays collected in the elemental peaks and the bremstrahlung. The resulting arrays representing x-ray or electron intensity are referred to here as x-ray or electron images. Thus, for example, the P image represents the intensity of the phosphorus peak at each point in the image.

Analogue raster analysis and digital image analysis provided related but complementary information in this study. Image analysis provided higher spatial resolution because of the better precision with which adjacent areas of analysis could be selected, particularly if the myofilaments were skewed. However, the greater number of subcellular regions sampled required a much longer sampling time for each sarcomere (~24 h for images compared with 1 h for static rasters) and only a few sarcomeres in a few fibers were sampled using images. In addition, since the hydrocarbon contamination occurring in some image sets over a 24-h period was significant, the bremstrahlung signals could not be used as an accurate measure of irradiated dry mass, and Ca concentrations could not be computed. In contrast, analogue rasters were used to sample selected subsarcomeric regions in a much larger number of sarcomeres from many fibers, allowing assessment of the statistical validity of the results for multiple sarcomeres, fibers, and Ca levels. In addition, the lower total electron dose in static raster analysis, along with use of a liquid nitrogen cooled anticontaminator, kept the hydrocarbon contamination to negligible levels, permitting computation of Ca dry mass concentrations.

Analogue raster analysis was carried out at room temperature using a side entry goniometer stage tilted 40° toward the detector. Anticontaminators above the diffusion pumps and surrounding the sample kept contamination of the sample to very low levels. A scan rotation device allowed orientation of the rectangular raster relative to the ultrastructure. The grid was oriented so that the fiber axis in a particular section was parallel to the tilt axis of the stage, and hence the striations were perpendicular to the tilt axis. This eliminated the geometrical problem of mixing of adjacent regions of analysis within the sarcomere when the stage was tilted to 40°. The diameter of the beam, under conditions normally used for analogue and digital analysis (5–12 nA), was estimated to be 50 nm. Rectangular rasters used in analogue raster mode were ~0.3 by 1 μm, were oriented with the long axis perpendicular to the fiber axis, and spanned the entire width of the sarcomere (see Data Collection Strategies below).

Support film spectra were collected adjacent to the section and were used to estimate the magnitude of corrections for both continuum and Ca x-ray counts contributed by the support film to each myofilament spectrum. Subtraction of Ca counts contributed by the support films resulted in average corrections of 0.47, 1.2, and 0.32 mmol/kg dry wt to A-band, I-band, and overlap regions, respectively. Approximately 20% of the data sets were rejected because film Ca corrections were deemed to be unacceptably high (resulting in >1.5 mmol/kg dry wt average Ca correction in the overlap region).

Spectra were processed using programs resident on the Link AN10000 (Statham, 1977). For each data set, the energy calibration was determined from the position of the copper peak in a representative spectrum. In addition, first derivatives of major peaks were included in the fit to correct further for energy calibration errors (Kitazawa et al., 1983). A digital top-hat filter (Schamber, 1976; Statham, 1977) was then applied to strip the peaks from the continuum. The filtered unknown spectrum was compared with a library of filtered standard peaks to derive the best linear least-squares fit. This procedure yielded peak and bremstrahlung (1.34–1.64 keV) integrals for the unknown spectrum. After correction for the contribution by the support film, the Ca peak counts so obtained were used for direct comparison of relative distributions of Ca within sarcomeres (see Figs. 2–4, *upper*, and Fig. 6). Alternatively, dry weight concentrations (e.g., for Ca) were computed by (*a*) normalizing the peak counts to the bremstrahlung counts, (*b*) multiplying by proportionality constants determined from protein and binary standards (Shuman et al., 1976), and (*c*) correcting for the difference in the average atomic number of the standard and that of the unknown. This correction factor is computed by an iterative procedure, beginning with elemental concentrations estimated from the spectral data and assuming that the elements are associated with a protein matrix. Corrections were made for beam-induced loss of the hydrocarbon matrix (Cantino et al., 1986).

Digital images were collected at room temperature in 128 × 128 × 16 bit arrays. To obtain quantitative information, we used a trackball or "mouse" to mask out the pixels in the desired region, and the same mask was applied to all of the images to extract the average counts per pixel (Wong et al., 1989). Simultaneous STEM images, though collected, were often poor in quality because of photomultiplier gain changes, so we used the S image as a guide to position masks in the appropriate regions of interest. Note that all x-ray images are acquired simultaneously, so positions of S and Ca images will be identical. Film Ca corrections were derived by collecting a 1000 second spectrum on the adjacent support film just before and just after digital analysis. The Ca correction in counts per pixel was computed by averaging the Ca counts from these spectra and normalizing for the difference in acquisition time between analogue raster analysis and single pixel digital analysis.

Specimen drift was minimal during both analogue raster and digital image analysis. During analogue raster analysis, the position of the raster was monitored several times during the acquisition. Drift was usually negligible over a 500-s spectral acquisition, but slight corrections in raster position were made when necessary. In digital images, collected over a 24–36-h period, drift was sometimes observed. Total drift during digital image collection was generally <0.50 μm. Since images were always oriented parallel to the fiber axis, each 128 pixel line sampled sequentially along an entire sarcomere. Drift would only affect our results if its magnitude during a single line were significant compared with the lateral dimension over which we averaged our digital image data (~150 nm). Over the entire duration of an image collection, this would correspond to a total drift of 19 μm, which is at least 10 times greater than any drift ever seen during our analyses.

Images typically were collected using 4–6 s per pixel dwell time, and data were averaged over bands comprising hundreds of pixels (typically 700–1,200). Data from three to four images were combined to produce each histogram in Figs. 2, 3, and 4. Since the specimen anticontaminator was not always cooled during the image acquisition, contamination of the section by hydrocarbons (but not Ca) sometimes occurred during analysis. For this reason, we did not attempt to compute dry weight concentrations from image data. Note that the contamination has no effect on the measurement of Ca counts, except in contributing additional random noise because of the increase in the continuum signal.

Data collection strategies

Paired sets of Ca counts (rather than dry mass concentrations) were used to estimate the distribution of Ca along the sarcomere, independent of the filament mass present at each point (this is discussed in more detail in Results). This procedure provides an unambiguous measure of relative Ca only if the following requirements are satisfied.

1. Each set of spectra must be collected from adjacent H-zone, I-band, and overlap regions of the same half sarcomere to assure that section thickness is constant for the three measurements.

2. Spectra within each set must be collected with the same total dose. This condition requires constancy of acquisition time, beam current, and raster size over the time needed to collect one complete set of spectra.

3. The density of each filament type (number of filaments per unit cross sectional area) must remain constant in H-zone, I-band, and overlap regions.

The first two requirements present relatively little difficulty. Section thickness is quite constant over a half sarcomere field (judging from similarity of continuum counts collected from the same regions of adjacent sarcomeres), and spectra within each set were always collected from the same half sarcomere. Spectra in each set were collected in sequence over a period of time $\leq$ 1 h, whereas the beam current, which was monitored using a Faraday cup mounted above the specimen, remained constant over periods of many hours.

The third requirement is less easily satisfied. A potential source of error in the analysis arises if the filament density (number of filaments per unit volume) changes from I-band to overlap zone. Observations from our freeze-dried cryosections indicate that in some cases, the myofibrillar diameter is up to 10% greater in the overlap zone than in the I-band (although the magnitude of the difference differs from fiber to fiber). A raster placed within the overlap zone will sample fewer filaments than will the same sized raster in the adjacent I-band, and the amount of Ca bound per unit length of filament in the overlap region may be underestimated relative to that in the I-band. On the other hand, if the scanning rasters are adjusted to different widths depending on the myofibrillar width, then the number of filaments sampled across is constant but the current density changes, leading to increased x-ray emission. If the raster is made to span the entire width of the overlap region but is kept constant, then this error can be corrected, at least in the plane of the section. This last approach was the collection strategy used in this study. Data from digital images are similarly corrected for filament density differences in the plane of the section, since the acquire time is proportional to the area sampled (data at each pixel are acquired over the same time interval).

The collection strategies described above will only ensure that no error occurs due to filament density differences in the plane of the section. Differences in the density of sampled filaments in the direction perpendicular to the plane of the section will also exist and can be expected to contribute up to 10% overestimation of Ca measured in the I-band relative to the overlap region. Note that this effect would tend to lead to an underestimation of any enhancement in the Ca distribution in the overlap region as compared with the I-band.

Data reduction and statistical errors

Several factors contribute to the observed variation in data from digital images. Pixel to pixel variation within a particular band in a single image will contain contributions from statistical fluctuations in the number of x rays emitted and collected (counting error), variations in the number computed in the filter and linear least-squares fit (fitting error), and actual variation in the amount of Ca present in the sample at each image point. The third is likely to be largely caused by inhomogeneity in the filament mass from one pixel to another. When N equivalent pixels are averaged together, the variation in the mean counts per pixel will be reduced by $1/\sqrt{N}$. To estimate the standard error associated with the sum of pixel counts ($= N \times$ mean counts/pixel), the pixel to pixel standard deviation within each band of each image was computed and multiplied by $N/\sqrt{N}$. To predict the pixel to pixel variation in the sum of pixels from several images, we added in quadrature the standard errors for equivalent bands of all images to yield the error bars shown in the upper portions of Figs. 2–4.

The predicted variation due to pixel to pixel differences described previously can be compared with the observed image to image variation among several images collected from the same section. This variation will include contributions from pixel to pixel variations but may also include intrinsic sarcomere to sarcomere variation and possibly as yet unidentified variations among data sets from different images (e.g., film correction errors). Since raw Ca counts will vary from image to image depending on local section thickness, beam current, and dwell time, comparisons between images can be made only if data from each image are normalized to some x-ray signal that has the same dependences. We chose to use the Na signal in the center of the overlap band (Na_o) for three reasons: the signal is large; the region is relatively homogeneous and easy to identify; and the Na signal in this region will reflect the same sarcomere to sarcomere differences in section thickness, average beam current, and acquire time as other bands in the same image. In each of Figs. 2–4 the lower half shows the mean Ca/Na_o ratio for each band with the error bar showing standard error of the mean for three to four images.

In general, the total width of the M-line mask was half that of the other masks, since data were contributed from only one M-line per sarcomere versus from bands in each of two half sarcomeres for each of the other regions. To correct for this inequity (effectively, a difference in acquisition time) and to allow the M-line Ca count to be directly compared with the other bands, we doubled the M-line Ca count before displaying it in Figs. 2–4.

To obtain calcium binding data corrected for the contributions from calcium binding to thick filaments (solid bars in Figs. 2–4), we subtracted the average number of counts measured in the nonoverlap A-band (H-zone) of the same sarcomeres from that measured in the overlap region. In transition regions between overlap and nonoverlap, half this amount was subtracted, since myofilament misalignment caused some filaments in this area to be in full overlap and some to have no overlap.

To test whether the amount of Ca (as measured using static rasters) was greater in the overlap region than in the I-band at each pCa, we compared Ca counts measured in each I-band with the counts measured in the adjacent overlap minus counts in the H-zone. Data from all fibers at each pCa were pooled. Statistical significance at each pCa level was determined using a paired two sample t test.

RESULTS

Subsarcomere variation in Ca binding: results from digital x-ray images

Digital x-ray images were used to characterize the distribution of Ca along the sarcomere. Fig. 1 shows an exam-

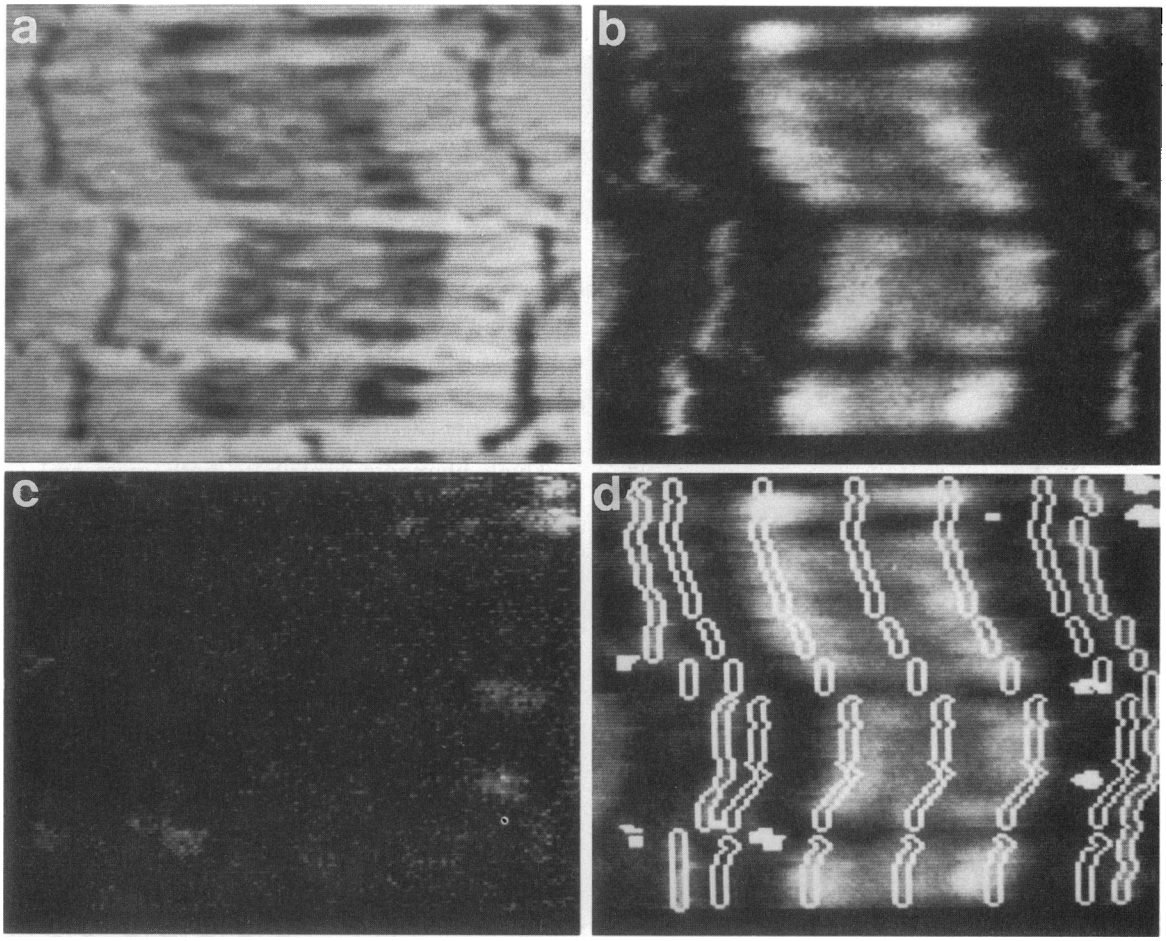

FIGURE 1 Digital electron and x-ray images of several sarcomeres in a freeze-dried cryosection of glycerinated rabbit psoas muscle. (*a*) 512 × 512 pixel digital transmission electron image, collected just before digital x-ray imaging. (*b*) S image. (*c*) P image. The P image was used to determine the location of possible SR fragments and to correct for any associated Ca. (*d*) Outlines of several masks overlaid on the S image.

ple of the images acquired and the procedure used to extract Ca data from them. A 512 × 512 pixel digital electron image (*a*) was collected before x-ray analysis. Comparison of *a* with the S image (*b*) collected over the next 24 h demonstrates the relatively small amount of drift that occurs during acquisition. The corresponding P image (*c*) represents the intensity of the phosphorus signal at each point in the image. Although some P is associated with the myofilaments, a much greater signal is generated by remnants of the membrane-bounded organelles disrupted by the skinning procedures. Since such remnants are not clearly identifiable in the S image and might bind Ca, we used the P image to identify membranous fragments and to correct for any Ca counts contributed by such fragments to the myofilament Ca counts. We found very little Ca associated with these remnants, and corrections were small. Fig. 1 *d* shows outlines of several myofilament masks overlaid on the original image. Masks were drawn as a series of bands stretching side to side across the entire sarcomere. Since Z-bands and M-lines were not in perfect register, a break in the masking pattern was placed just before the Z-band, and the Z-band mask was drawn separately to give better alignment between the mask and the ultrastructure. For this reason, the data shown in Figs. 2–4 have a gap at the end of the I-band. The first band in each figure represents the relative counts collected from such regions as shown in Fig. 1 *c* (putative SR membranes).

Fig. 2 shows data obtained from four images of a fiber frozen at pCa 6.25. The measured Ca rises dramatically in the region of overlap between thick and thin filaments. At pCa 5.31 (Fig. 3), the amount of Ca was also somewhat enhanced in the overlap region, although the relative difference between I-band and overlap region is not as dramatic as at pCa 6.25. At pCa 4.76 (Fig. 4) the disparity between the I-band and the overlap region is still less pronounced.

Note that in the normalized histograms (lower parts of Figs. 2–4) each image was given equal weight in the computed mean, whereas in the upper histograms, images

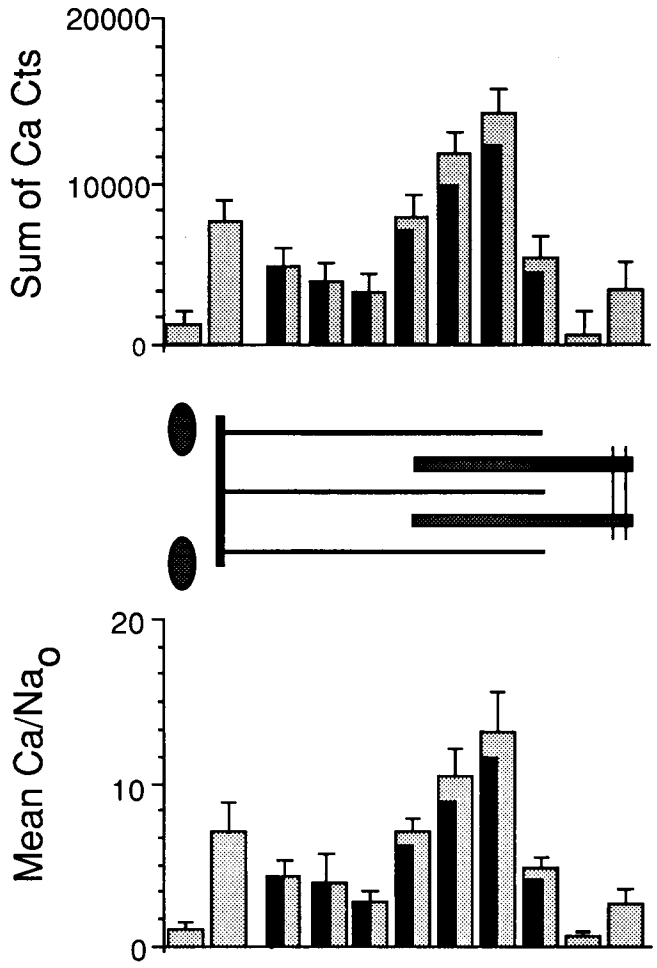

FIGURE 2 Data from four sarcomeres of a fiber frozen at pCa 6.25. The upper plot shows the sum of Ca counts (corrected for film Ca) from corresponding bands of the sarcomeres in the four images. The error bars are computed as described in Methods. Each band is vertically aligned with its corresponding position in the half sarcomere; the shaded ovals at the left-hand side represent remnants of the sarcoplasmic reticulum. The Ca data shown in the lower part of the figure have been normalized to the Na value at the center of each overlap region in each of the four sarcomeres. The error bars represent standard errors of the mean of data from four images. The shaded bars in both upper and lower histograms represent total Ca at each position in the sarcomere; the solid bars show the net Ca levels along the thin filaments after the estimated contribution from Ca^{2+} binding to thick filaments is subtracted (see Methods).

with higher numbers of counts contributed proportionally more to the total Ca count. This difference accounts for some of the relative differences in bar height and sign between upper and lower portions of each figure.

Subsarcomere variations in Ca dry weight concentration

Because concentrations of Ca could not be accurately computed from digital images and because we wished to evaluate statistically the elevation of Ca counts in the overlap region, we compared analogue raster data collected from 17 fibers: 3 fibers at pCa 9.05, 3 at pCa 6.25, 2 at pCa 5.67, 2 at pCa 5.31, 5 at pCa 4.76, and 2 at pCa 4.30. 9 to 11 spectra were collected from each fiber. Dry weight concentrations were derived from spectral data as described in Methods. For each subsarcomeric region, the dry weight concentrations for all sarcomeres at a given pCa were pooled and averaged. The standard error of the mean of all sarcomeres at each pCa was also computed. The data from H-zone (H), I-band (I), and overlap (O) regions are displayed in Fig. 5.

Subsarcomere variations in Ca binding per unit thin filament dry mass

Thick filaments contribute both mass and Ca to the measured dry weight concentration of Ca reported for the overlap region. The added mass accounts for the greater concentration of Ca in the I-band than in the overlap region (Fig. 5). To compare directly the amount of Ca localized to thin filaments in the I-band and in the

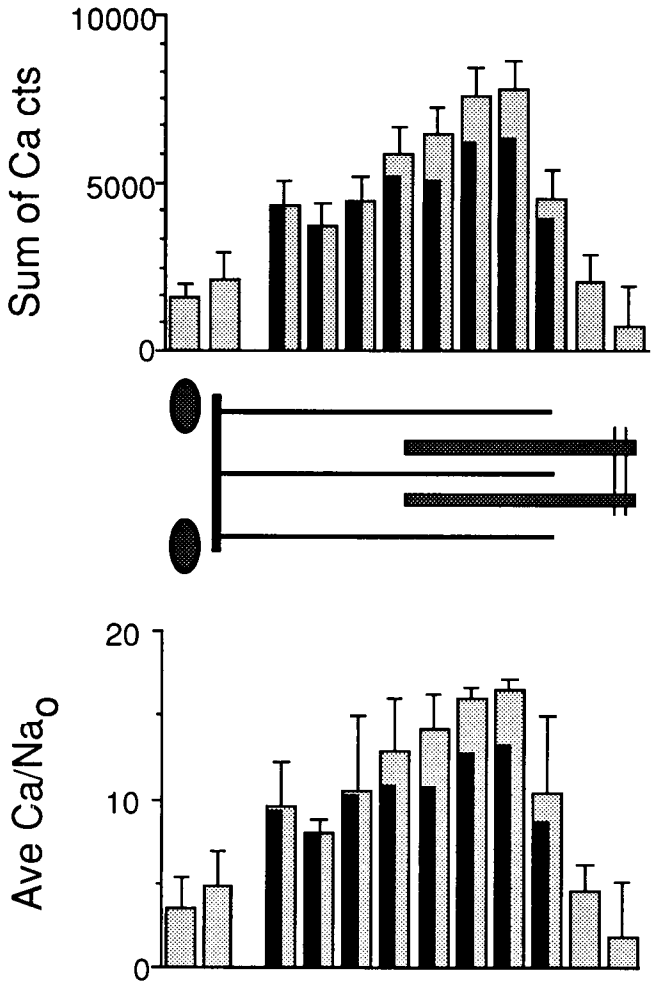

FIGURE 3 Data from three images of sarcomeres from a fiber frozen at pCa 5.31. Shaded and solid bars and error estimates are as in Fig. 2.

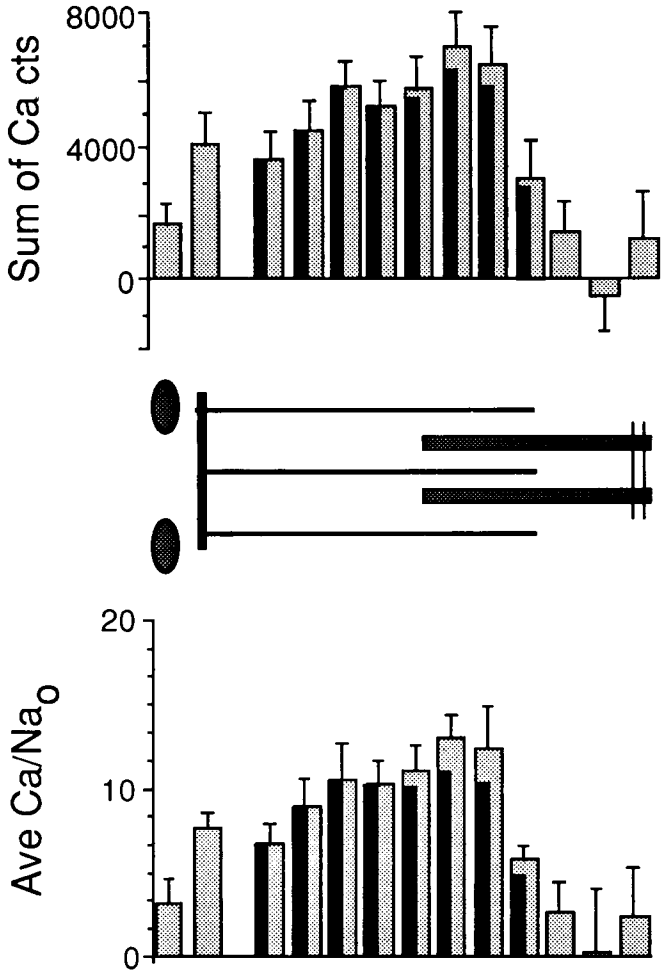

FIGURE 4 Data from four images of sarcomeres from a fiber frozen at pCa 4.76. Shaded and solid bars and error estimates are as in Fig. 2.

overlap region, we examined the peak Ca counts in adjacent I-band and overlap regions obtained from the spectra described previously but without normalization to dry mass. In addition, we subtracted from the peak Ca counts detected in the overlap region our best available estimate of Ca bound to thick filaments. The rectangular shape of the analogue rasters, in combination with myofilament skew in some of the sarcomeres sampled, precluded collection of data from solely that region of the H-zone containing myosin heads. We thus chose to estimate the amount of Ca bound to thick filaments by measuring the Ca localized to the central region of the H-zone, a region including the M-line, the bare zone, and a narrow portion containing myosin heads. The spatial resolution afforded by digital image analysis allowed us to test whether Ca counts detected in the central region of the H-zone differed from those in the peripheral region, away from the M-line and the bare zone. No significant difference was detected in images collected at the pCa values examined: 6.25, 5.31, and 4.76.

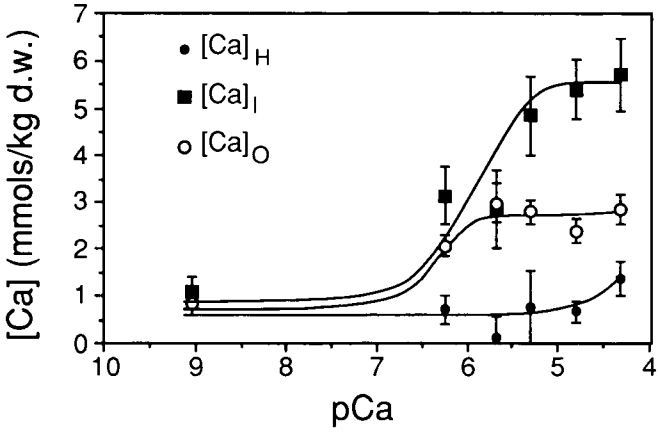

FIGURE 5 Calcium concentrations in mmol/kg dry wt in the H-zone (H), I-band (I), and overlap (O) regions of 17 fibers. Error bars show standard error of the mean.

Thus, for each set of sarcomeres, the contribution of Ca bound to thin filaments in the overlap region, Ca_{Io}, was estimated as the difference between the sum of Ca counts measured in the overlap zone and the sum of counts measured in the center of the H-zone:

$$Ca_I = \sum_{\substack{\text{all}\\ \text{spectra}}} Ca\ cts_I,$$

$$Ca_H = \sum_{\substack{\text{all}\\ \text{spectra}}} Ca\ cts_H, \quad Ca_O = \sum_{\substack{\text{all}\\ \text{spectra}}} Ca\ cts_O,$$

and the portion of the Ca signal attributable to Ca bound to thin filaments in the overlap region was estimated as:

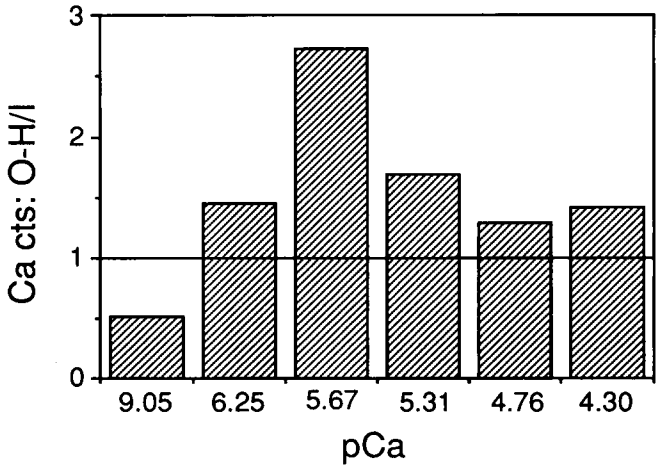

FIGURE 6 Ratios of the sum of counts from the overlap region (corrected for H-zone counts) to I-band counts from the same sarcomeres at six different values of pCa. A ratio of one indicates equal Ca levels in overlap and nonoverlap regions of the I-band, whereas ratios greater than one indicate enhanced Ca levels in the overlap region in the presence of rigor cross-bridges.

TABLE 2 **Statistical summary of count difference tests**

pCa	n (spectra)	Mean Ca ct difference ($Ca_{Io} - Ca_I$)	SEM	*P* (one sided)
9.05	39	−38	48	NS
6.25	31	82	49	0.05
5.67	20	161	40	<0.001
5.31	18	141	82	0.05
4.76	40	62	40	0.06
4.30	29	100	58	0.05

NS, not significant.

$$Ca_{Io} = Ca_O - Ca_H.$$

The sum of Ca counts over all sarcomeres for overlap, H-zone, and I-band was used to compute a single Ca_{Io}/Ca_I ratio at each pCa (Fig. 6). Note that the statistical variation in this ratio is highest at pCa 9.05 because the Ca counts are very low. We tested whether Ca_{Io} was significantly greater than Ca_I at each pCa using a paired *t* test, with values paired sarcomere by sarcomere. Table 2 summarizes the results.

The Ca_{Io}/Ca_I ratios in Fig. 6 can be multiplied by $[Ca]_I$, the average I-band Ca concentrations computed from the same sarcomeres at each pCa (Fig. 5). The resulting values, $[Ca]_{Io}$, can be interpreted as estimates of the concentrations of Ca per unit mass of thin filament in the overlap region in mmol/kg thin filament mass:

$$[Ca]_{Io} = [Ca]_I \frac{Ca_{Io}}{Ca_I}.$$

Fig. 7 compares the average $[Ca]_{Io}$, $[Ca]_I$, and $[Ca]_H$ measured at each pCa. Since the method used to compute Ca_{Io}/Ca_I ratios yields a single value at each pCa, no estimate of the standard error in $[Ca]_{Io}$ values has been computed (refer to Table 2 for the statistical significance of differences in Ca counts).

To determine whether our data were consistent with the known Ca^{2+} binding properties of troponin, we used the measured dry weight concentrations of Ca to estimate the corresponding number of moles of Ca bound per mole of troponin. If only actin, tropomyosin and troponin are assumed to be present in the I-band (mole ratio 7:1:1, mol wt 42.3, 68, and 80 kD, respectively) (Yates and Greaser, 1983) and then each Ca bound to troponin would contribute 2.25 mmol/kg dry wt of thin filament Ca, giving a total of 9.01 mmol/kg dry wt if four Ca are bound per troponin. However, it is now generally accepted that other accessory proteins are present in the I-band, notably titin and nebulin. A similar calculation including contributions by titin and nebulin can be made using relative fractions (mass per unit of myofibrillar dry mass) of 0.22, 0.05, 0.05, 0.10, and 0.05 for actin, tropomyosin, troponin, titin, and nebulin, respectively (Bailey, 1948; Wang, 1982; Yates and Greaser, 1983). Nebulin is assumed to be distributed evenly along the thin filament and nowhere else in the sarcomere (Maruyama et al., 1989). Titin is assumed to be distributed evenly from M-line to Z-line at rest length but is assumed to stretch only in the I-band when the sarcomere length is increased to 3.2 μm (Maruyama et al., 1985; Itoh et al., 1988). With these assumptions, the total I-band mass of actin, tropomyosin, troponin, nebulin, and titin (in kilograms per mole of troponin) can be estimated. Inclusion of titin and nebulin in the computation lowers the contribution of each mole of Ca to the $[Ca]_I$ or $[Ca]_{Io}$ value to 1.7 mmol/kg dry wt or a total of 6.8 mmol/kg dry wt for occupancy of the four sites of TnC with Ca^{2+}. This estimate should be viewed as a lower limit, since any proteolysis of labile proteins such as titin will raise the observed dry mass concentrations of Ca. Thus, the amount of binding we estimate for the I_o region (Fig. 7) appears to be most consistent with the binding of four Ca per troponin.

DISCUSSION

The discovery of troponin as the Ca^{2+}-sensitive switch for contraction in skeletal muscle was soon followed by the observation that the binding of Ca^{2+} to troponin is modulated by actomyosin interaction. Two questions have arisen concerning this modulation: (*a*) do rigor linkages unmask an additional Ca^{2+} binding site per troponin in fibers and (*b*) does the cooperativity invested in the thin filament allow rigor linkages in the overlap region of the thin filament to modulate the binding of Ca^{2+} to troponin in the I-band? Our results, which represent the first direct and spatially resolved measurements of the Ca distribution along the length of the thin filament, can be evaluated in the context of these two questions.

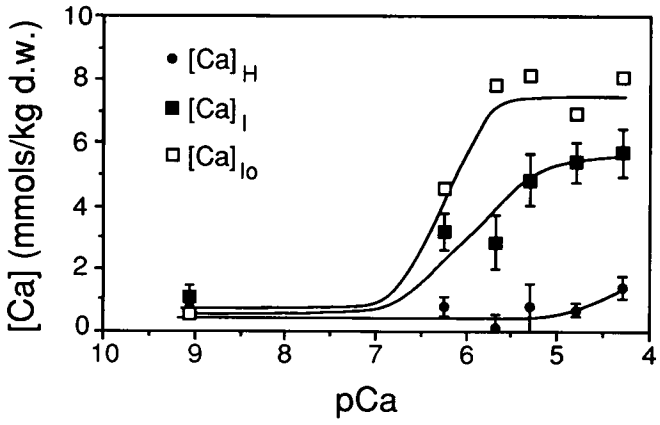

FIGURE 7 Ca concentration in the H-zone ($[Ca]_H$), the I-band ($[Ca]_I$), and the overlap region of the I-band, corrected for the mass and Ca contributions of the thick filaments ($[Ca]_{Io}$). Error bars show standard errors of the mean for $[Ca]_I$ and $[Ca]_H$ (see text).

Modulation of the Ca binding relation

In their study of ^{45}Ca binding to thin filaments, Bremel and Weber (1972) found that the formation of rigor linkages, both in myofibrils and in reconstituted actomyosin preparations, appreciably increases the affinity of troponin for Ca^{2+}. Their observation has been corroborated by other studies. Rosenfeld and Taylor (1985), using reconstituted thin filaments in which the troponin I had been fluorescently labeled, found that saturation of thin filaments with myosin subfragment 1 in the absence of MgATP leads to an increase of 5–10-fold in the Ca^{2+} affinity of the two low-affinity Ca^{2+} binding sites of TnC. Assaying the amount of ^{45}Ca bound to demembranated ventricular muscle, Pan and Solaro (1987) found that the formation of rigor linkages increases the Ca^{2+}-affinity of the low-affinity class of site of cardiac TnC three- to fourfold. Data from similar experiments with demembranated skeletal fibers, however, suggested that the formation of rigor linkages leads to an unmasking of an additional Ca^{2+} binding site per troponin, yielding a total of four sites per troponin in the overlap region yet only three per troponin in the I-band (Fuchs, 1977*a, b*). Using EPXMA, we reexamined the effect of the formation of rigor linkages in demembranated fibers.

Unlike ^{45}Ca binding assays, EPXMA offers a spatial resolution that allows quantitation of Ca distributions along the length of myofilaments in individual sarcomeres. Since total Ca in the bathing solution is below the detection limit for our instrumentation (see Methods), the most reasonable interpretation of the distributions reported here is that they represent Ca bound to the myofilaments. Digital images of the subsarcomeric Ca distribution at pCa 6.25 reveal that Ca localized to the overlap region, even when corrected for the estimated amount of Ca bound to thick filaments, prominently exceeds Ca localized to the I-band. Because the difference between Ca counts in the overlap region and in the I-band diminishes at lower pCa values, these data support the view that the formation of rigor linkages increases the affinity of TnC for Ca^{2+}. It is of particular interest to determine whether this difference persists at saturating levels of free Ca^{2+}, since such a result would suggest that formation of rigor linkages also leads to the unmasking of an additional Ca^{2+} binding site. Unfortunately, no definitive answer can be obtained from the digital images, given the statistical variability in the measurements and the limited sample population.

Data from analogue raster analyses of an appreciable number of fibers provide a more discriminating test of the effects of rigor linkages. At subsaturating concentrations of free Ca^{2+}, Ca counts in the overlap region, when corrected for Ca bound to the thick filaments, are significantly higher than Ca counts in the I-band. The excess Ca counts in the overlap region diminishes when a saturating free Ca^{2+} concentration is attained; however, the difference retains borderline statistical significance ($P \leq 0.06$ at pCa 4.76 and 4.30). Thus, the data from the analogue raster analyses support conclusions not only of an increase in Ca^{2+} affinity of TnC but also of a possible unmasking of an additional Ca^{2+} binding site as mediators of the Ca enhancement in the overlap region. Although consistent with an increase in the Ca^{2+}-affinity of TnC and possibly in the number of binding sites per TnC in the overlap region, our data cannot exclude the possibility that there is also an increase in the apparent cooperativity of Ca^{2+} binding (e.g., see Fuchs, 1977*b*; Grabarek et al., 1983).

Implicit in the preceding discussion is the assumption that the increase in Ca measured in the overlap region results from an increase in Ca^{2+} binding to TnC. That the increased localization is due to Ca^{2+} binding to the thin filaments does seem tenable: the concentration of Ca^{2+} per kilogram dry weight of thin filament in the overlap region is consistent with the binding of 4 mol Ca^{2+}/mol TnC at saturation, which is compatible with the known binding capacity of TnC from rabbit psoas muscle (Potter and Gergley, 1975). A second possibility that must be considered is that the increased Ca signal might arise from Ca bound to sites on the thick filaments. This seems unlikely at high values of pCa, since Fuchs and Black (1980) have demonstrated that myosin binds little or no Ca^{2+} in the presence of millimolar concentrations of free Mg^{2+} at pCa values of 5 and higher. Moreover, we have estimated the binding of Ca to myosin and have subtracted this estimate from our measurements of Ca in the overlap region. We cannot, on the other hand, rule out the possibility that the distribution of Ca bound along the length of the thick filament at low values of pCa (<5.0) is nonuniform and that our correction based on the Ca measured in the center of the H-zone is unrepresentative of Ca bound to myosin heads in the overlap region. Results from the digital images analyzed so far show no consistent difference between Ca measured in the center of the H-zone and in that part of the H-zone containing myosin heads. It remains possible that more Ca binds to rigor cross-bridges in the overlap region than to myosin heads in the H-zone, i.e., that actomyosin interaction enhances Ca^{2+} binding both to troponin and to the Ca^{2+}-Mg^{2+} binding site of the myosin regulatory light chain. Hofmann and co-workers (1990) present evidence that myosin light chain two may modulate the number of cross-bridges formed during Ca^{2+} activation in skinned rabbit psoas muscle.

Cooperativity along the thin filament

Brandt and collaborators (1984*a, b*, 1987) hypothesized that all 26 troponin-tropomyosin units of a regulatory strand make a concerted, cooperative transition from the inhibited, or off, position to the disinhibited, or on, position. Their hypothesis stems from the observation that the removal of <5% of TnC from fibers, correspond-

ing to ~1 TnC on average per regulatory strand, significantly reduces the cooperativity apparent in the tension-pCa relation. Supporting the hypothesis, results from a further study (Brandt et al., 1990) revealed that the cooperativity apparent in the relation between tension and MgATP concentration in the absence of Ca^{2+} likewise decreases on the removal of a minimal amount of TnC from fibers. On the basis of the hypothesis, it might be anticipated that modulation by rigor linkages of Ca^{2+} binding to the thin filament in the overlap region should extend along the entire length of the thin filament. Data from the analogue raster analyses contradict the anticipated result: the amount of Ca estimated to be bound to thin filaments in the overlap region of the sarcomere significantly exceeds the amount of Ca localized in the I-band. Corroborating the analogue raster analyses, digital images of Ca distributions within the sarcomere at pCa 6.25 also show significantly enhanced Ca in the overlap region (corrected for Ca^{2+} binding to thick filaments) compared with the I-band. Although there are insufficient data to characterize precisely the relation between enhanced Ca localization and distance from the A-I junction toward the Z-band, the images of fibers frozen at pCa 6.25 suggest that the enhanced Ca localization decays within the first mask (0.15 μm) after the A-I junction. This distance corresponds to the length of about four tropomyosin-troponin units along a regulatory strand. After the initial decay, the distribution of Ca binding in the I-band appears to be relatively constant.

The discrepancy between our observations and the hypothesis could arise for at least two reasons: (*a*) our experiments evaluated the cooperativity of the thin filament in relation to Ca^{2+} binding and not to tension development and (*b*) our experiments were performed in the absence of MgATP. No study thus far has compared directly the cooperativity in Ca^{2+} binding to the regulatory sites of TnC with the cooperativity in tension development. Suggestive of a difference is the observation of Grabarek et al. (1983) that the cooperativity in the MgATPase activity-pCa relation exceeds the cooperativity in the fluorescence-pCa relation determined with a fluorescent derivative of TnC in reconstituted thin filaments. Allen et al. (1992) noted that the cooperativity apparent in the tension-pCa relation is significantly greater than the cooperativity in the fluorescence-pCa relation determined with labeled TnC incorporated into single fibers with a sarcomere length of 2.4 μm. It remains conceivable that some of the cooperativity apparent in the tension-pCa relation originates from the thick filament, for example from the presence of two myosin heads per myosin molecule.

Our observation of a limited spatial spread along the thin filament of the modulatory effect of rigor linkages on Ca^{2+} binding has parallels in studies performed with myofibrils and with native and reconstituted thin filaments. Swartz et al. (1990) observed that, in the absence of Ca^{2+}, fluorescently labeled myosin subfragment 1 (S1), at low concentrations relative to actin, preferentially bound to sites in the overlap region of the A-band in myofibrils from skeletal muscle fibers in rigor. The lack of binding to sites along thin filaments in the I-band suggests that rigor linkages exposed S1 binding sites only in the overlap region. The authors also noted that this effect extended for only two to three regulatory units beyond the A-I junction. Tobacman and Sawyer (1990), studying Ca^{2+} binding to native and reconstituted cardiac thin filaments, interpreted their results as indicating that Ca^{2+} is fourfold less likely to bind to TnC within a sequence of inhibited units than to bind to TnC adjacent to a sequence of disinhibited units. Wegner and Walsh (1981) analyzed the interactions of tropomyosin-troponin I-troponin T and tropomyosin-halotroponin with reconstituted actin filaments and found that the generation of a sequence of tropomyosin-troponin units in either the inhibited or the disinhibited form was fourfold less likely than the elongation of an existing sequence. Using an equation describing the equilibrium between helical and randomly coiled conformations in polypeptides, Wegner and Walsh calculated that the average number of tropomyosin-troponin units in a sequence of adjacent units in the same regulatory state is three at the midpoint in the transition between total inhibition and total disinhibition of a regulatory strand. This calculation is compatible with our observation of a limited spread along the thin filament for the enhancement in Ca^{2+} binding induced by rigor cross-bridges in the overlap region.

SUMMARY

The spatial resolution afforded by EPXMA allowed detection of the Ca distribution along the length of myofilaments within single sarcomeres. Data from digital images and analogue raster analyses revealed that the amount of Ca in the overlap region prominently exceeds the amount of Ca in the I-band at subsaturating concentrations of free Ca^{2+} and that the excess Ca in the overlap region diminishes, but remains detectable, at saturating concentrations. The data thus suggest that the formation of rigor linkages exerts multiple effects on the binding of Ca^{2+} to thin filaments in the overlap region by increasing the affinity of TnC for Ca^{2+} and possibly by unmasking additional Ca^{2+} binding sites. Moreover, data from the digital images show that the cooperativity invested in the thin filament is insufficient to allow appreciable propagation of Ca enhancement into the I-band.

We are grateful for the expert technical assistance of Ms. Shellee Cunnington, Ms. Su Wan Chen, and Ms. Linda Wilkinson for preparation of freeze-dried cryosections and for assisting with data collection and analysis, to Ms. Robin Coby for assisting with the mixing of solutions, and to Ms. Martha Mathiason, who helped to coordinate communications between coauthors in three states. We especially thank Dr. Dale

E. Johnson for his many helpful suggestions and for encouraging the use of quantitative x-ray imaging in this project.

This work was supported by National Institutes of Health grants P01-HL-31962, K04-HL-02142, and GM-07270.

Received for publication 17 April 1992 and in final form 11 September 1992.

REFERENCES

Allen, D. G., and S. Kurihara. 1982. The effects of muscle length on intracellular calcium transients in mammalian cardiac muscle. *J. Physiol. (Lond.)*. 327:79–94.

Allen, T. StC., L. D. Yates, and A. M. Gordon. 1992. Ca^{2+}-dependence of structural changes in troponin-C in demembranated fibers of rabbit psoas muscle. *Biophys. J.* 61:399–409.

Bailey, K. 1948. Molecular weight of tropomyosin from rabbit muscle. *Biochem. J.* 43:271–281.

Brandt, P. W., M. S. Diamond, and F. H. Schachat. 1984*a*. The thin filament of vertebrate skeletal muscle co-operatively activates as a unit. *J. Mol. Biol.* 180:379–383.

Brandt, P. W., M. S. Diamond, B. Gluck, M. Kawai, and F. Schachat. 1984*b*. Molecular basis of cooperativity in vertebrate muscle thin filaments. *Carlsberg Res. Commun.* 49:155–167.

Brandt, P. W., M. S. Diamond, J. S. Rutchik, and F. H. Schachat. 1987. Co-operative interactions between troponin-tropomyosin units extend the length of the thin filament in skeletal muscle. *J. Mol. Biol.* 195:885–896.

Brandt, P. W., D. Roemer, and F. H. Schachat. 1990. Co-operative activation of skeletal muscle thin filaments by rigor crossbridges. *J. Mol. Biol.* 212:473–480.

Bremel, R. D., and A. Weber. 1972. Cooperation within actin filament in vertebrate skeletal muscle. *Nature (Lond.)*. 238:97–101.

Cantino, M. E., L. E. Wilkinson, M. K. Goddard, and D. E. Johnson. 1986. Beam induced mass loss in high resolution biological microanalysis. *J. Microsc. (Oxf.)*. 144:317–327.

Chiu, Y., J. Asayama, and L. E. Ford. 1982. A sensitive photoelectric force transducer with a resonant frequency of 6 kHz. *Am. J. Physiol.* 243:C299–C302.

Ebashi, S., and M. Endo. 1968. Calcium ion and muscle contraction. *Prog. Biophys. Mol. Biol.* 18:123–183.

Ellis, K. J., and J. F. Morrison. 1982. Buffers of constant ionic strength for studying pH dependent processes. *Methods Enzymol.* 87:405–425.

Fink, R. H. A., D. G. Stephenson, and D. A. Williams. 1986. Potassium and ionic strength effects on the isometric force of skinned twitch muscle fibres of the rat and toad. *J. Physiol. (Lond.)*. 370:317–337.

Fuchs, F. 1977*a*. The binding of calcium to glycerinated muscle fibers in rigor. *Biochim. Biophys. Acta.* 491:523–531.

Fuchs, F. 1977*b*. Cooperative interactions between calcium-binding sites on glycerinated muscle fibers. The influence of cross-bridge attachment. *Biochim. Biophys. Acta.* 462:314–322.

Fuchs, F. 1978. On the relation between filament overlap and the number of calcium-binding sites on glycerinated muscle fibers. *Biophys. J.* 21:273–277.

Fuchs, F. 1985. The binding of calcium to detergent-extracted rabbit psoas muscle fibres during relaxation and force generation. *J. Muscle Res. Cell Motil.* 6:477–486.

Fuchs, F., and B. Black. 1980. The effect of magnesium ions on the binding of calcium ions to glycerinated rabbit psoas muscle fibers. *Biochim. Biophys. Acta.* 622:52–62.

Fuchs, F., and Y. Wang. 1991. Force, length, and Ca^{2+}-troponin C affinity in skeletal muscle. *Am. J. Physiol.* 261:C787–C792.

Gordon, A. M., R. E. Godt, S. K. B. Donaldson, and C. E. Harris. 1973. Tension in skinned frog muscle fibers in solutions of varying ionic strength and neutral salt composition. *J. Gen. Physiol.* 62:550–574.

Gordon, A. M., E. B. Ridgway, L. D. Yates, and T. Allen. 1988. Muscle cross-bridge attachment: effect on calcium binding and calcium activation. *Adv. Exp. Med. Biol.* 226:89–98.

Grabarek, Z., J. Grabarek, P. C. Leavis, and J. Gergely. 1983. Cooperative binding to the Ca^{2+}-specific sites of troponin C in regulated actin and actomyosin. *J. Biol. Chem.* 258:14098–14102.

Guth, K., and J. D. Potter. 1987. Effect of rigor and cycling crossbridges on the structure of troponin C and on the Ca^{2+} affinity of the Ca^{2+}-specific regulatory sites in skinned rabbit psoas fibers. *J. Biol. Chem.* 262:13627–13635.

Hall, T. A., and B. L. Gupta. 1982. Quantification for the x-ray microanalysis of cryosections. *J. Microsc. (Oxf.)*. 126:333–345.

Hellam, D. C., and R. J. Podolsky. 1969. Force measurement in skinned muscle fibers. *J. Physiol. (Lond.)*. 200:806–819.

Hofmann, P. A., and F. Fuchs. 1987. Effect of length and cross-bridge attachment on Ca^{2+} binding to cardiac troponin C. *Am. J. Physiol.* 253:C90–C96.

Hofmann, P., J. M. Metzger, M. L. Greaser, and R. L. Moss. 1990. Effects of partial extraction of light chain 2 on the Ca^{2+} sensitivities of isometric tension, stiffness, and velocity of shortening in skinned skeletal muscle fibers. *J. Gen. Physiol.* 95:477–498.

Itoh, Y., T. Suzuki, S. Kimura, K. Ohashi, H. Higuchi, H. Sawada, T. Shimizu, M. Shibata, and K. Maruyama. 1988. Extensible and less-extensible domains of connectin filaments in stretched vertebrate skeletal muscle sarcomeres as detected by immunofluorescence and immunoelectron microscopy using monoclonal antibodies. *J. Biochem. (Tokyo)*. 104:504–508.

Johnson, D. E., and M. E. Cantino. 1986. High resolution biological x-ray microanalysis of diffusable ions. *In* Advanced Techniques in Biological Electron Microscopy. Vol. 3. J. Koehler, editor. Springer-Verlag, Berlin. 73–100.

Khoo, R. H., R. W. Ramette, C. W. Culberson, and R. G. Bates. 1977. Determination of hydrogen ion concentrations in seawater from 5 to 40°C; standard potentials at salinities from 20–45%. *Anal. Chem.* 49:29–34.

Kitazawa, T., H. Shuman, and A. P. Somlyo. 1982. Calcium and magnesium binding to thin and thick filaments in skinned muscle fibres: electron probe analysis. *J. Muscle Res. Cell Motil.* 3:437–454.

Kitazawa, T., H. Shuman, and A. P. Somlyo. 1983. Quantitative electron probe analysis: problems and solutions. *Ultramicroscopy.* 11:251–262.

Martell, A. E., and R. M. Smith. 1974. Critical Stability Constants. Vols. I and II. Plenum Publishing Corp., New York. 469 pp. and 415 pp.

Martell, A. E., and R. M. Smith. 1982. Critical Stability Constants. Vol. V. Plenum Publishing Corp., New York. 604 pp.

Maruyama, K., T. Yoshioka, H. Higuchi, K. Ohashi, S. Kimura, and R. Natori. 1985. Connectin filaments link thick filaments and z-lines in frog skeletal muscle as revealed by immunoelectron microscopy. *J. Cell Biol.* 101:2167–2172.

Maruyama, K., A. Matsuno, H. Higuchi, S. Shimaoka, S. Kimura, and T. Shimizu. 1989. Behaviour of connectin (titin) and nebulin in skinned muscle fibers released after extreme stretch as revealed by immunoelectron microscopy. *J. Muscle Res. Cell Motil.* 10:350–359.

O'Sullivan, W. J., and G. W. Smithers. 1979. Stability constants for

biologically important metal ligand complexes. *Methods Enzymol.* 63:294–336.

Pan, B., and R. J. Solaro. 1987. Calcium-binding properties of troponin C in detergent-skinned heart muscle fibers. *J. Biol. Chem.* 262:7839–7849.

Phillips, R. C., P. George, and R. J. Rutman. 1963. Potentiometric studies of the secondary phosphate ionizations of AMP, ADP and ATP and calculations of thermodynamic data for the hydrolysis reactions. *Biochemistry.* 2:501–508.

Phillips, R. C., P. George, and R. J. Rutman. 1966. Thermodynamic studies of the formation and ionization of magnesium (II) complexes of ADP and ATP over the pH range of 5 to 9. *J. Am. Chem. Soc.* 88:2631–2640.

Potter, J. D., and J. Gergely. 1975. The calcium and magnesium binding sites on troponin and their role in the regulation of myofibrillar adenosine triphosphatase. *J. Biol. Chem.* 250:4628–4633.

Ridgway, E. B., and A. M. Gordon. 1984. Muscle calcium transient: effect of post-stimulus length changes in single muscle fibers. *J. Gen. Physiol.* 83:75–103.

Rosenfeld, S. S., and E. W. Taylor. 1985. Kinetic studies of calcium and magnesium binding to troponin C. *J. Biol. Chem.* 260:242–251.

Schamber, F. H. 1976. Proc. Symp. X-ray Fluorescence Anal. Environ. Samples, 241–257.

Shuman, H., A. V. Somlyo, and A. P. Somlyo. 1976. Quantitative electron probe microanalysis of biological thin sections: methods and validity. *Ultramicroscopy.* 1:317–339.

Somlyo, A. V., A. P. Somlyo, and H. Shuman. 1989. Electron-Probe X-ray-Microanalysis of Ca^{2+}, Mg^{2+} and other ions in rapidly frozen cells. *Methods Enzymol.* 172:203–229.

Statham, P. J. 1977. Deconvolution and background subtraction by least-squares fitting with prefiltering of spectra. *Anal. Chem.* 49:2149–2154.

Swartz, D. R., M. L. Greaser, and B. B. Marsh. 1990. Regulation of binding of subfragment 1 in isolated rigor myofibrils. *J. Cell Biol.* 111:2989–3001.

Trybus, K. M., and E. W. Taylor. 1980. Kinetic studies of the cooperative binding of subfragment 1 to regulated actin. *Proc. Natl. Acad. Sci. USA.* 77:7209–7213.

Tobacman, L. S., and D. Sawyer. 1990. Calcium binds cooperatively to the regulatory sites of the cardiac thin filament. *J. Biol. Chem.* 265:931–939.

Wang, K. 1982. Purification of titin and nebulin. *Methods Enzymol.* 85:264–274.

Wegner, A., and T. P. Walsh. 1981. Interaction of tropomyosin-troponin with actin filaments. *Biochemistry.* 20:5633–5642.

Wong, J. G., L. Wilkinson, S. W. Chen, K. Izutsu, D. Johnson, and M. Cantino. 1989. Quantitative analysis of elemental images. *Scanning.* 11:12–19.

Yates, L. D., and M. L. Greaser. 1983. Quantitative determination of myosin and actin in rabbit skeletal muscle. *J. Mol. Biol.* 168:123–141.